

Improving Corrosion Protection of Urethane Acrylate UV Curable Coatings Derived from Palm Oil via Graphene Oxide Particle Incorporation

(Peningkatan Perlindungan Kakisan Salutan Uretana Akrilat Pengawetan UV daripada Minyak Sawit melalui Penggabungan Zarah Oksida Grafena)

MOHD SOFIAN ALIAS^{1,4}, RABIAHTUL ZULKAFLI², NORINSAN KAMIL OTHMAN^{1,*}, MOHD SUZEREN MD. JAMIL³, SITI RADIAH MOHD KAMARUDIN⁴, SITI FATAHIYAH MOHAMAD⁴, MOHD HAMZAH HARUN⁴, MAHATHIR MOHAMED⁴ & MAZNAH MAHMUD⁴

¹*Materials Science Programme, Department of Applied Physics, Universiti Kebangsaan Malaysia, 43600 UKM Bangi, Selangor, Malaysia*

²*Department of Earth Sciences and Environments, Faculty of Science and Technology, Universiti Kebangsaan Malaysia, 43600 UKM Bangi, Selangor, Malaysia*

³*Department of Chemical Sciences, Faculty of Science and Technology, Universiti Kebangsaan Malaysia, 43600 UKM Bangi, Selangor, Malaysia*

⁴*Malaysian Nuclear Agency, Bangi, 43000 Kajang, Selangor, Malaysia*

Received: 14 October 2024/Accepted: 12 November 2024

ABSTRACT

This study explores the enhancement of corrosion protection properties in urethane acrylate UV-curable coatings derived from palm oil through the incorporation of graphene oxide particles (GOP). GOP were added into palm oil-based urethane acrylate (POBUA) using a sonication technique. The performance of POBUA with the influence of GOP was determined using Thermal Gravimetric analysis (TGA) and Field Emission Scanning Electron Microscopy (FESEM). Meanwhile, the corrosion testing was confirmed by electrochemical testing of Electrochemical Impedance Spectroscopy (EIS). TGA demonstrated that the presence of GOP a coating additive, improved the coating in the POBUA, enabling better heat absorption. This is because more energy was required to break the polymer chain during decomposition. Additionally, EIS showed that the diffusion of corrosive ions was hindered due to the tortuous pathways created by the GOP within the POBUA network. The highest Rct value of POBUA coating with 0.5 wt% GOP give 99.64% corrosion protection for mild steel which significantly improved compared to neat POBUA coating which only 63.6% corrosion protection. Furthermore contact angle analysis showed the presence of GOP improved hydrophobicity properties of POBUA coating contributing to their excellent corrosion resistance. These findings highlight the potential of POBUA/GOP curable coatings for providing effective protection of mild steel surfaces.

Keywords: Corrosion protection; graphene oxide particles; palm oil; UV curable coating

ABSTRAK

Penyelidikan ini meneliti penambahbaikan sifat perlindungan kakisan dalam salutan penyembuhan UV uretana akrilat yang berasal daripada minyak sawit (POBUA) melalui penggabungan zarah oksida grafina (GOP). GOP telah ditambah ke dalam uretana akrilat minyak sawit menggunakan teknik sonikasi. Prestasi POBUA dengan pengaruh GOP telah ditentukan menggunakan analisis gravimetri termal (TGA) dan mikroskopi imbasan elektron imbasan medan (FESEM). Sementara itu, ujian kakisan disahkan melalui ujian elektrokimia iaitu spektroskopi impedans elektrokimia (EIS). TGA menunjukkan bahawa kehadiran GOP dalam salutan POBUA meningkatkan penyerapan haba, kerana lebih banyak tenaga diperlukan untuk memecahkan rantai polimer semasa penguraian. Selain itu, EIS menunjukkan bahawa penyebaran ion kakisan terhalang disebabkan oleh laluan berliku yang dicipta oleh GOP dalam rangkaian POBUA. Nilai Rct tertinggi bagi salutan POBUA dengan 0.5 wt% GO memberikan perlindungan kakisan optimum iaitu sebanyak 99.64% berbanding salutan POBUA yang hanya memberikan 63.6% perlindungan kakisan terhadap keluli lembut. Selain itu, analisis sudut sentuhan menunjukkan kehadiran GOP meningkatkan sifat hidrofobik salutan POBUA. Penemuan ini menonjolkan potensi salutan POBUA/GOP sebagai salutan perlindungan karat bagi permukaan keluli lembut.

Kata kunci: Minyak sawit; perlindungan karat; salutan penyembuhan UV; zarah gentian oksida

INTRODUCTION

Recent technological advancements and growing knowledge have spurred the development of novel coating materials to meet contemporary human needs. Given the critical role of surface protection in preventing material loss and safeguarding human life, researchers have focused on creating sustainable coating materials, particularly for corrosion protection. Numerous studies have conclusively demonstrated the efficacy of plant-based green sources in mitigating corrosion on steel substrates (Yahya, Othman & Ismail 2019; Zulkafli et al. 2014). The increasing regulatory pressure to reduce volatile organic compounds (VOCs) and the diminishing petroleum reserves have intensified the search for corrosion protection resins derived from renewable sources and green technologies (Alam et al. 2014). One promising development in this area is the creation of a UV-curable corrosion protection coating based on palm oil, which offers a potential alternative to traditional petrochemical-based resins due to its high production volume and lower VOC content (Khattoon et al. 2021).

Previous studies have investigated the use of palm oil-based resins in UV-curable coatings, often incorporating additives to enhance specific properties. Other research demonstrated that the addition of silica particles can improve scratch resistance and hardness by strengthening the polymer matrix (Nik Salleh et al. 2011; Said et al. 2013). Research on palm oil-based urethane acrylate (POBUA) coatings showed that silica can also enhance hydrophobicity (Harun 2021). Similarly, silicon dioxide has the ability to reduce water absorption and improve water repellency in palm oil-based resins (Mustapha et al. 2022). Wan Rosli et al. (2003)'s study on UV-curable coatings containing epoxidised palm oil and cycloaliphatic diepoxide showed that higher epoxide concentrations can reduce hardness and gel content, but the inherent polymerizability of palm oil provides a strong foundation for corrosion protection.

Meanwhile, to increased corrosion resistance and thermal barrier coating Ahmed et al. (2020) also developed the eco-friendly coating from palm oil-based resin and nano-silica particles by using heating curing. In this study, the best results for heat resistance testing and TAFEL plot came from the sample containing 0.6% silica. The results indicates no visible cracks at 140 °C with corrosion rate value 0.0328 mmy. Although this formulation has potential applications in industrial coatings but a long time of heating for curing and usage of solvent in formulation give limitation for costing and environment purposed.

Despite these advancements, research on palm oil-based corrosion protection coatings remains limited. Alias et al. (2022) investigated the effects of graphite particles on the corrosion protection properties of POBUA coatings and found that graphite can increase corrosion resistance by blocking the permeation of corrosive agents. However, the natural characteristics of graphite, such as weak Van der

Waals forces, can lead to softening and potential weakening of the polymer composite (Sengupta et al. 2011). To address this, graphene oxide particles (GOP) have been proposed as a more promising additive. Previous research has shown that GOPs can effectively block the infiltration of corrosive agents, improve anticorrosion properties, enhance cathodic protection, and induce hydrophobicity in the polymer matrix (Di et al. 2016; Ding et al. 2018; Prolongo et al. 2014).

The current study aimed to develop an eco-friendly, green corrosion protection coating by incorporating graphene particles into palm oil-based urethane acrylate resin. The UV curing process and the influence of varying GOP percentages on the coating's performance are thoroughly analysed using various scientific methods. The role of GOP in enhancing the corrosion resistance of POBUA coatings on mild steel surfaces is carefully investigated, contributing to the advancement of sustainable corrosion protection technologies.

MATERIALS AND METHODS

Commercial mild steel containing (in wt.%) 0.001 wt.% P, 0.045 wt.% Al, 0.187 wt.% Si, 0.586 wt.% Mn, 0.486 wt.% C, 0.004 wt.% S, and 98.691% iron (Fe) were received and cut into pieces. Palm oil-based urethane acrylate (POBUA), supplied from Nuclear Malaysia, was used as received without further modification. Furthermore, graphene oxide particles as a filler in POBUA were obtained from Timesnano. Meanwhile, the photoinitiator Irgacure 184, which is chemically known as alpha-hydroxy ketone, was purchased from Sigma Aldrich. POBUA resin and GOP were combined in an amber bottle and stirred at 300 rpm for 2 h. The POBUA/GOP formulations were then sonicated using a VCX500 sonicator (Sonics & Materials, USA) at a power of 500 W and a frequency of 20 kHz. The sonication was performed with an amplitude setting of 50% and a pulse mode set to pause for 1 s every 2 s, over a total duration of 10 min. The formulations were stored for 24 h at 27 °C before being coated onto 4 cm × 4 cm mild steel plates using a K Hand Coater, resulting in a 50 µm thick wet film. The coatings were cured under 22 s of UV irradiation using 20 cm IST UV machine with a conveyor speed of 10 m/min and a current of 8A at intensity 200 W/cm. The cured films were peeled off for subsequent spectroscopic, thermal, and mechanical characterisation.

The influence of GOP in POBUA coating and curing process under UV irradiation was observed and monitored using FTIR spectrophotometry (Spectrum 2000, Tensor II Bruker). Each recorded spectrum was obtained with 32 scans at a resolution of 4.0 cm⁻¹, covering a wavenumber range from 500 to 4000 cm⁻¹. Particle analyser (Honeywell, microtrac X100) was used to characterize particle size distribution of GOP. X-ray powder diffractometer (XRD) (PANalytical, X'Pert PRO MPD PW 3040/60) that operates with a Ni-filtered Cu K α radiation ($\lambda = 0.15418$

nm) demonstrated the crystallinity regions in POBUA/graphene oxide. The samples were scanned with 2θ values ranging from 5° to 60° . The Segal equation was adapted to produce the POBUA/graphene oxide crystallinity index. Meanwhile, all curable film coatings were examined by TGA model TG 209 F3 Tarsus Netzsch and FESEM model Carl Zeiss/GeminiSEM 500, respectively. Before probing under FESEM, platinum was used to coat the sample to prevent charging. Furthermore, the wetting behaviour of curable coating was evaluated using the contact angle. The measurements were taken in triplicate and at room temperature of $30 \pm 2^\circ\text{C}$.

The corrosion behaviour of the coatings is assessed by electrochemical measurement tests using EIS containing 3.5% NaCl using Reference 600 Potentiostat/Galvanostat/ZRA (Gamry Instruments, USA). The impedance of the coating was measured during the testing with a three-electrode system. The surface area of the exposed coated steel was 1 cm^2 . For the EIS measurements, an open circuit potential of 10 mV RMS sinusoidal amplitude and 10 points per decade was used, which covered a frequency ranging from 0.01 Hz to 100 kHz.

RESULTS AND DISCUSSION

Figure 1 shows the overlay FTIR spectra for cured coating of POBUA, POBUA + 0.1% GOP, POBUA + 0.5% GOP and POBUA + 0.8% GOP. The intensity of $3600 - 3100\text{ cm}^{-1}$ regions increased relates to the overlapping of the -NH and -OH stretching vibration which present in POBUA + GOP coating. Previous study showed formation of graphene was produces carboxyl groups bonding (Ar-COOH) on graphene surfaces due to cleavage of aromatic C-C bonds during nitric acid oxidation (Radovic et al. 2017). Hence, the sharp peak at $1700 - 1730\text{ cm}^{-1}$ is ascribed to C=O of carboxylic and ketone groups of GOP and POBUA, respectively. Furthermore, the small peak around $1560\text{ cm}^{-1} - 1600\text{ cm}^{-1}$ which associated with C=O stretching or N-H bending vibrations could explain the hydrogen bonding formation between the N-C=O group in POBUA and the OH groups from GOP. The polarity of hydrogen atom bridge the N-C=O group in POBUA and the OH group from GOP via inter H-bonding as illustrated in Figure 3. Previous studies have demonstrated that the extensive surface area of graphene oxide promotes favorable hydrogen bond formation with polyurethane (Liu et al. 2015). XRD analysis was conducted to investigate the impact of GO on the crystallinity of POBUA coatings. The resulting diffraction patterns, shown in Figure 2, showed a broad, amorphous halo characteristic of POBUA coatings. Meanwhile The addition of GO enhanced the crystallinity of POBUA, likely due to the formation of nucleation sites by the GO particles. GO, a two-dimensional graphene derivative, has been shown to increase polymer nucleation density, leading to smaller and more numerous crystalline regions (Jang, Oh & Lee 2021). The long-

chain acrylate structure of POBUA and its crosslinking network contribute to its crystallinity. Previous studies have indicated that longer polymer segments exhibit better crystallinity, potentially due to reduced segment mobility (Nissenbaum, Greenfeld & Wagner 2020). However, increased crystallinity may compromise certain coating properties, such as surface adhesion.

The incorporation of GO into the POBUA matrix enhances crystallinity by increasing packing density and providing nucleation sites through its surface functional groups (OH, COOH) (Jang, Oh & Lee 2021). As the GO content increases, the amorphous halo intensity decreases, and a sharp peak appears at $2\theta = 26.4^\circ$, corresponding to the (002) crystallographic planes of graphite structures. This shift in the diffraction peak is consistent with previous findings (Sang et al. 2018). Figure 1 also illustrates the correlation between GO content and the crystallinity index (CI) of the cured POBUA film.

TGA was employed to evaluate the thermal properties of POBUA coatings containing varying amounts of GO. Figure 4 presents the thermograms of pristine POBUA and POBUA/GO coatings in a nitrogen atmosphere, and Table 1 summarizes the residue composition. The decomposition of pure POBUA coatings occurred in two stages: evaporation of photoinitiator, monomer, and solvent ($120-200^\circ\text{C}$) and pyrolysis of the polymer chains ($250-400^\circ\text{C}$) (Ariffin et al. 2020). The addition of GO increased the decomposition temperature, indicating improved heat resistance. This enhancement is attributed to GO's ability to improve thermal stability and facilitate heat dissipation through conductive pathways (Yu et al. 2021). The interaction between the POBUA matrix and the oxygen-containing functional groups on GO creates a more uniform distribution within the polymer. Additionally, due to its high aspect ratio and layered structure, GO forms a tortuous path in the polymer matrix. Figure 5 indicate the GOP size distribution analysis. The homogeneous phase of the POBUA-GO composite reduces the risk of micro-cracks and establishes a more robust crosslinked network, thereby enhancing matrix interaction and slowing the degradation of the polymer coating. This observation aligns with the findings of Thanh (2022) who reported that GO particles impede the penetration of heat and oxygen into the structure of alkyd chains, effectively reducing thermal decomposition. Furthermore, the intermolecular interactions between GO and POBUA hinder polymer chain movement, contributing to the higher decomposition temperature.

The sonication technique ensured uniform dispersion of GO within the POBUA matrix (Mellado et al. 2019). The residue percentage from TGA analysis correlated with the GO content. However, beyond 0.5 wt.% GO, there was no significant increase in decomposition temperature. This may be due to GO agglomeration, which reduces its effective volume fraction and hinders heat absorption and transfer (Huang et al. 2020).

The effectiveness of coating application of GOP and film properties was analysed through the morphology of mild steel surfaces. Meanwhile, contact angle measurements were conducted to assess the surface affinity of POBUA coatings with and without GOP. Figure 6 presents the FESEM images and CA of POBUA coatings and with varying GOP content (0.1-0.8 wt.%). The FESEM image of POBUA coating (Figure 6(a)) exhibited a small, dark pores appear as white circles, originating from the mild steel substrate and covered by the POBUA coating. This indicates that the POBUA coating is sufficiently thick to conceal the surface roughness of the mild steel. A smooth surface without delamination, indicating a strong interface between POBUA and mild steel. This is likely due to the polar groups in POBUA, which enhance adsorption and physical integrity (Mahidashti, Shahrabi & Ramezanzadeh 2018). As shown in Figure 6(b)-6(d), the surface morphology shifts from smooth to dense and rough when GOP content exceeds 0.8 wt.%. The increase in GOP content promotes aggregation and agglomeration within the POBUA coating, resulting in rougher and denser surfaces. This effect is likely attributed to the strong Van der Waals forces and hydrogen bonding between graphene oxide particles (Pourhashem et al. 2017). Previous studies have demonstrated that graphene oxide agglomeration occurs at concentrations exceeds 0.25 wt% (Rajabi, Rashed & Zaarei 2015).

Figure 6(e)-6(h) illustrates the CA value of POBUA with varying percentages of GOP. The POBUA exhibited hydrophobic behavior with a CA of 111° . A CA below 90° indicates wettability, while a value above 90° signifies

hydrophobicity (Sarkar et al. 2020). The hydrophobicity of POBUA is attributed to its crosslinked network structure, which reduces chemical affinity towards water molecules (Seo et al. 2011). Steric hindrance from bulky groups in palm oil-derived molecules further prevents intermolecular interactions between water and POBUA. These factors lead to water droplet on POBUA coatings. The hydrophobicity of coatings is crucial for corrosion protection, as hydroxyl groups are components of corrosive agents (Nam et al. 2015). The addition of GO slightly increased the contact angle, with the highest value observed at 0.1 wt.% GO. This is likely due to GO filling pores in the POBUA coating, enhancing surface irregularity and polymer structure. At low concentrations, graphene oxide particles (GOP) become well-embedded within the polyurethane (POBUA) matrix, which hides their oxygen-containing functional groups within the coating. This reduced exposure of polar groups and leads to an increase in the contact angle of the POBUA coating. Furthermore, the well-embedded GOP creates a smoother surface, which avoids interaction with water droplets by minimizing surface energy. Additionally, at low GOP levels, the regions of carbon atoms with more hydrophobic characteristics dominate the surface interactions, further enhancing the coating's hydrophobicity. However, at higher GO concentrations (0.5 wt.% and above), the CA decreased. This is attributed to GO agglomeration, which creates a rougher surface with increased contact area and water trapping (Sandhyarani, Prasadrao & Rameshbabu 2014). This result improved wettability and can make the surface more hydrophilic, which reduces water contact angles and increases hydrophobicity initially.

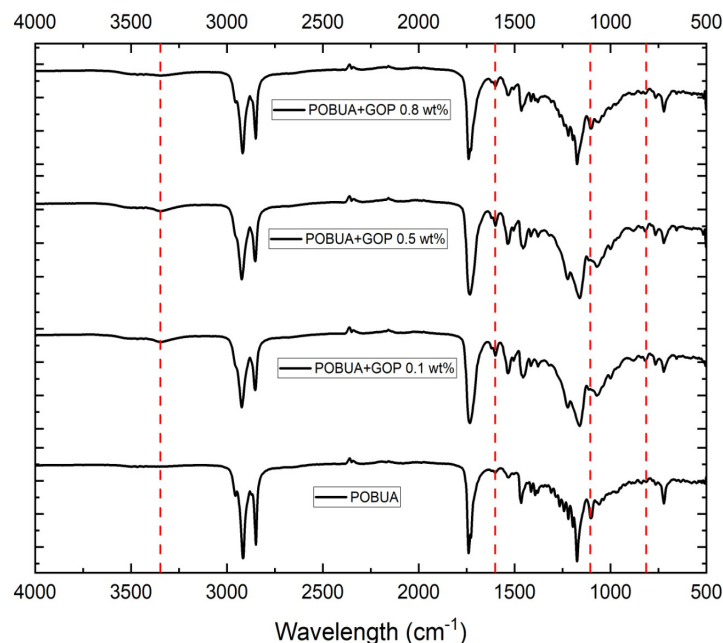


FIGURE 1. Overlay FTIR spectra for cured coating of POBUA, POBUA + 0.1% GOP, POBUA + 0.5% GOP and POBUA + 0.8% GOP

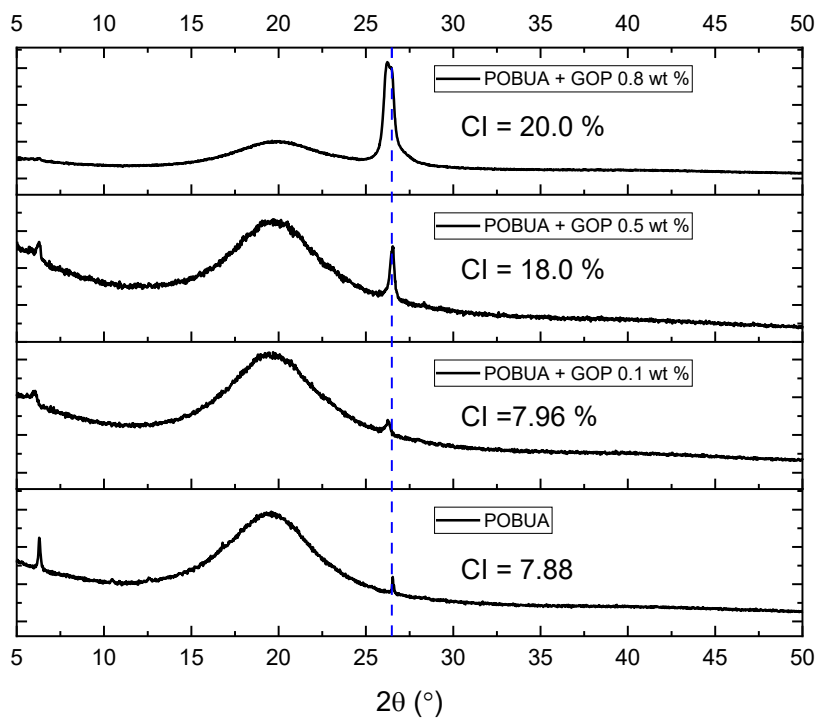


FIGURE 2. XRD graph of POBUA and POBUA with 0.1-0.8 wt% GOP

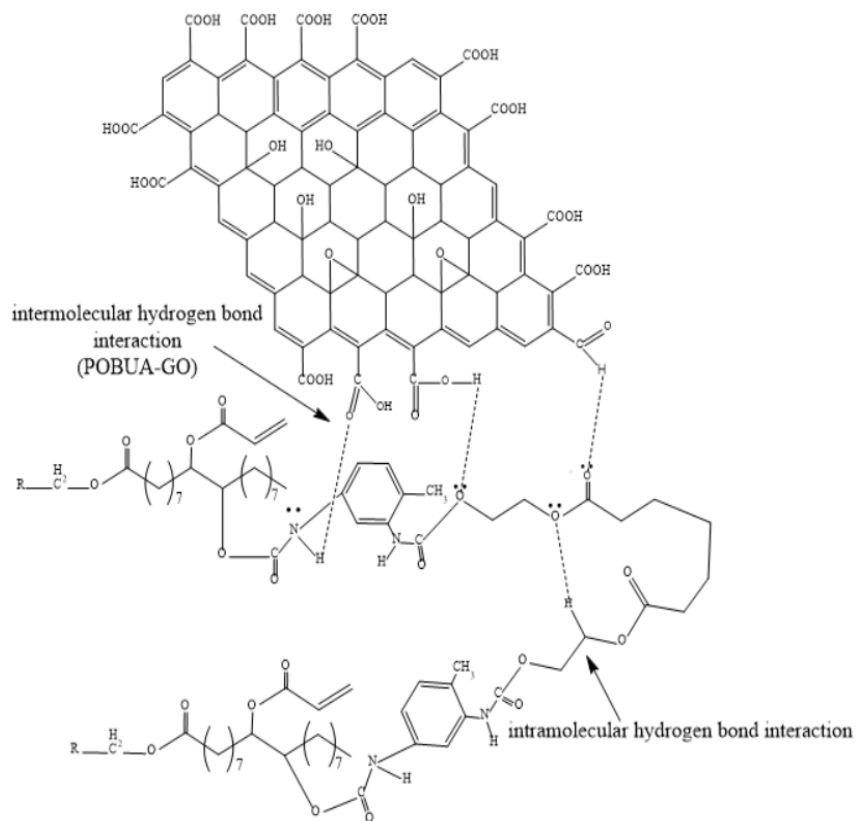


FIGURE 3. Hydrogen bonding from N-C=O group in POBUA and the OH group from GOP

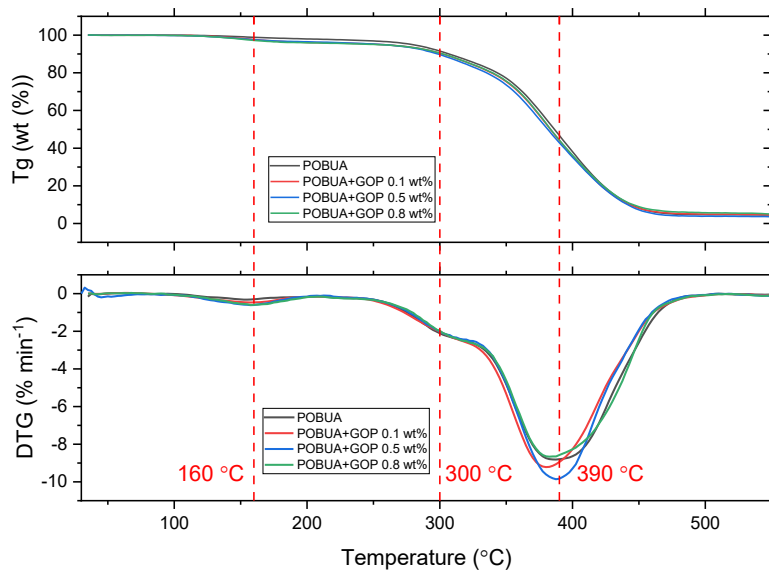


FIGURE 4. TGA curves of the POBUA and POBUA/GOP cured coatings

TABLE 1. TGA decomposition residue of POBUA at different GOP percentage

Sample	Decomposition temperature	
	T_{onset}	Residue wt. %
POBUA	310	0.15
POBUA + GOP 0.1 wt - %	347	3.85
POBUA + GOP 0.5 wt - %	342	4.12
POBUA + GOP 0.8 wt - %	342	5.12

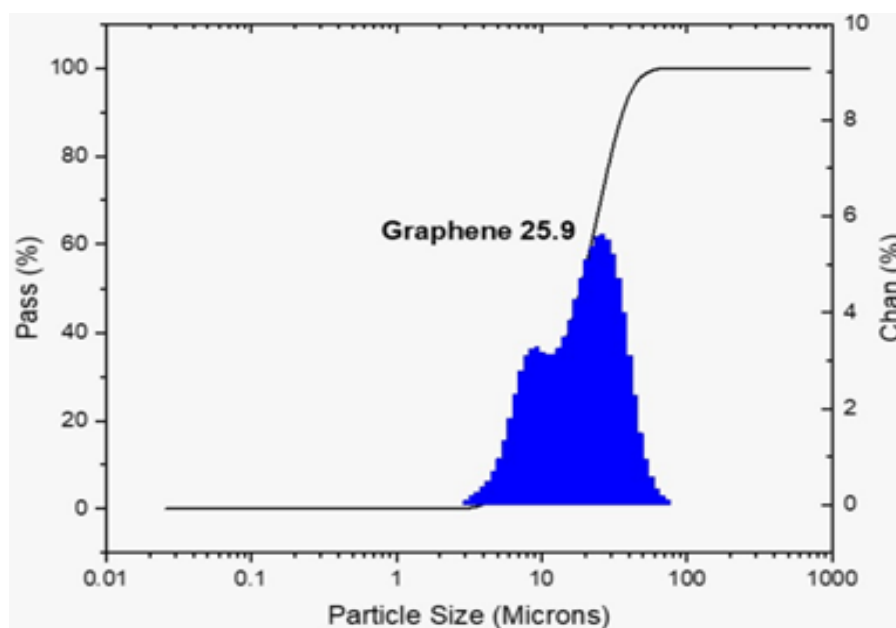


FIGURE 5. GOP size distribution analysis

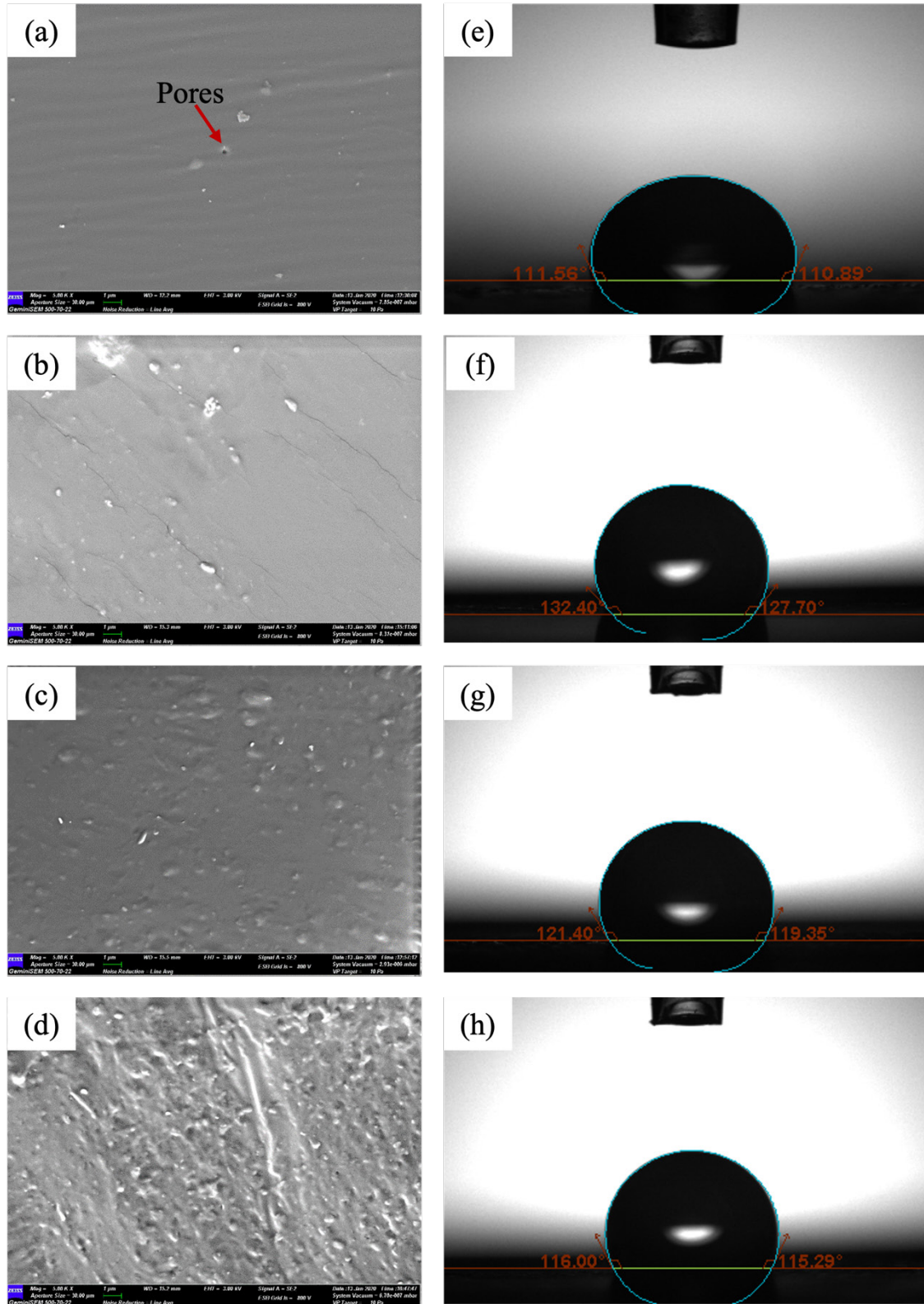


FIGURE 6. FESEM image for (a) POBUA, (b) POBUA + 0.1 wt.% GOP, (c) POBUA + 0.5 wt.% GOP, (d) POBUA + 0.8 wt.% GOP and CA value of (e) POBUA, (f) POBUA + 0.1 wt.% GOP, (g) POBUA + 0.5 wt.% GOP, (h) POBUA + 0.8 wt.% GOP coatings

Figure 7 presents the Nyquist and Bode plots of POBUA coatings with varying GO content, illustrating the corrosion resistance of mild steel. Two time constants in each plot indicate electrolyte infiltration through pores and cracks, leading to corrosion. The second time constant corresponds to corrosion at low frequencies (Suleiman et al. 2020). The second loop in the Nyquist curve represents the corrosion process after the formation of a passive layer, resulting from the reaction between the electrolyte and the mild steel surface. Table 2 shows the recorded coating resistance (R_c) values, with higher values for POBUA coatings containing 0.5 wt.% and 0.8 wt.% GO compared to the blank POBUA coating. This indicates improved corrosion protection. The charge transfer resistance (R_{ct}) values follow a similar trend, reaching their highest values for POBUA coatings with 0.5 wt.% and 0.8 wt.% GO. This finding is consistent with previous studies that suggest GO enhances corrosion protection (Pourhashem et al. 2017). Initially, low Q_c values (representing water diffusion) correlate with high R_{ct} values. However, after electrolyte infiltration, charge transfer activity leads to a decrease in R_{ct} . The increased GO content in the POBUA matrix hinders the penetration of corrosive agents, increasing the diffusion path length and resulting in larger Nyquist

semicircles. The percentage of corrosion protection can be calculated using Equation (1) as follows:

$$\text{Percentage of protection (\%)} = \frac{R_{ct} - R_{ct^0}}{R_{ct}} \times 100 \quad (1)$$

Well-distributed GO in the POBUA matrix is believed to reduce porosity, preventing electrolyte infiltration and enhancing corrosion resistance (Kumar et al. 2021). Furthermore, GO particles, with their layered structure, create a tortuous path for ions and water molecules attempting to penetrate the POBUA coating. This complex pathway increases the distance that corrosive ions, such as chloride ions, must travel to reach the metal substrate consequently slowing down ion diffusion and enhanced metal corrosion protection. The coating capacitance (Q_c) values, reflect water movement within the coating (Zuo et al. 2008). Water penetration can lead to coating delamination. The lowest Q_c values were observed at a GO content of 0.5 wt.%, followed by an increase at 0.8 wt.%. This is attributed to GO agglomeration, which creates porous regions allowing electrolyte diffusion (Cubides & Castaneda 2016).

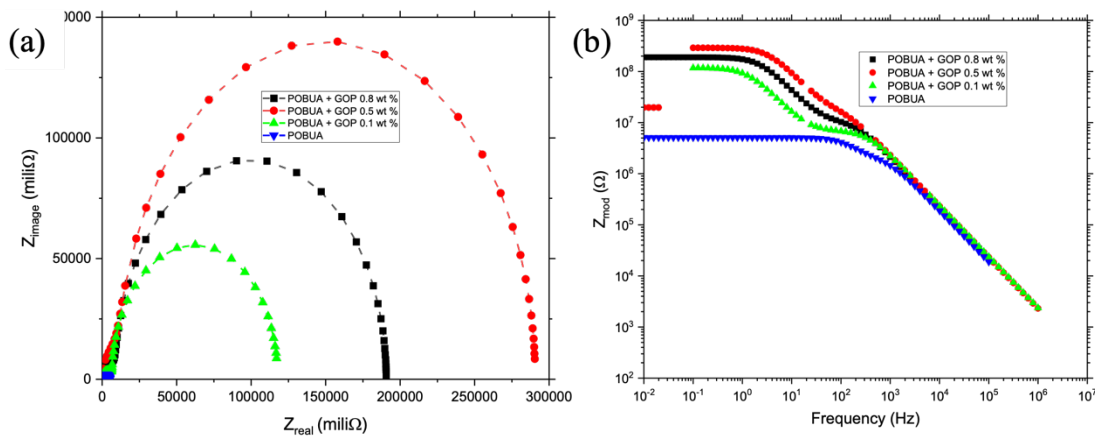


FIGURE 7. Electrochemical test of (a) Nyquist fitted and (b) Bode plots for the blank POBUA and POBUA/GOP coatings with different percentages of GOP

TABLE 2. Absolute value of R_c , R_{ct} , Q_c and percentages of corrosion protection

	$R_c(10^6)$ [Ωcm]	$R_{ct}(10^6)$ [Ωcm]	$Q_c (10^{12})$ [Fcm^{-2}]	$Q_{dl} (10^{-9})$ [Fcm^{-2}]	Corrosion protection [%]
Mild steel	8.77	0.92			
POBUA	2.579	2.528	84.28	0.417	63.6
POBUA+ GOP 0.1 wt%	7.359	110.5	67.23	1.063	99.16
POBUA+ GOP 0.5 wt%	30.12	260.5	68.78	111.8	99.64
POBUA+ GOP 0.8 wt%	13.19	177.4	73.35	323.3	99.48

The Bode plot in Figure 7(b) illustrates the corrosion resistance behavior. The impedance modulus increases with increasing GO content, with the highest value observed at 0.5 wt.% GO. Blank POBUA and POBUA with 0.1 wt.% GO exhibit significantly lower resistance values. This suggests that GO reduces porosity and creates a tortuous pathway within the polymer matrix, hindering electrolyte diffusion (Huang et al. 2012). A resistance value above $108 \Omega \text{ cm}^2$ indicates good protective properties, while values below $106 \Omega \text{ cm}^2$ suggest inadequate corrosion protection (Scully & Hensley 1994). The Bode plot shows two phases, representing the two stages of the corrosion process at the coating-electrolyte interface. While 0.5 wt.% and 0.8 wt.% GO are beneficial for corrosion resistance, excessive GO content (0.8 wt.%) can negatively impact coating performance. The charge transfer resistance (R_{ct}) values for coated and uncoated mild steel substrates with and without GO are denoted as R_{ct} and R_{oct} , respectively.

CONCLUSION

The integration of graphene oxide (GO) into POBUA coatings improves crystallinity and thermal stability by augmenting nucleation sites and packing density. XRD study demonstrates a decrease in amorphous halo intensity and the emergence of a distinct diffraction peak with elevated GO concentration, signifying improved crystallinity. The TGA data indicate enhanced heat resistance with the addition of GO; however, no substantial improvements are noted beyond 0.5 wt.% due to GO agglomeration. Analysis of surface morphology indicates that increased GO content results in rougher surfaces, while contact angle measurements imply that GO promotes hydrophobicity up to 0.1 wt.%, but diminishes it at elevated concentrations due to agglomeration. Corrosion resistance studies, demonstrated by Nyquist and Bode plots, indicate enhanced performance at GO concentrations up to 0.8 wt.%, with 0.5 wt.% producing optimal results due to diminished porosity and electrolyte penetration. Excessive GO content may compromise coating performance by elevating porosity and diminishing hydrophobicity. Further investigation could focus on exploring the effects of varying UV curing conditions on the performance of the GO-enhanced POBUA coating, as well as testing the coating's corrosion protection capabilities in more aggressive environments (acidic and alkaline environment).

ACKNOWLEDGEMENTS

The authors would like to acknowledge the Public Services Department (JPA) for sponsoring author education on this research under the JPA student scholarship. The authors also would like to thank the Ministry of Education Malaysia for the financial support through the research grant FRGS/1/2020/TK0/UKM/02/35. Furthermore, the authors also sincerely thank the Malaysian Nuclear Agency for providing the equipment and technical support, which made this work possible.

REFERENCES

- Alam, M., Akram, D., Sharmin, E., Zafar, F. & Ahmad, S. 2014. Vegetable oil based eco-friendly coating materials: A review article. *Arabian Journal of Chemistry* 7(4): 469-479.
- Alias, M.S., Othman, N.K., Kamarudin, S.R.M., Harun, M.H., Mohamed, M., Saidin, N.U., Mohamad, S.F. & Samsu, Z. 2022. Influence of graphite particles in UV-curable corrosion protection coating from palm oil based urethane acrylate (POBUA). *Industrial Crops and Products* 187: 115436-115451.
- Ahmed, B., Suhaila, N., Anbalagan, M.A., Hossen, M.D., Yunus, R. & Abdullah, A. 2020. Formulation of heat resistant paint from palm oil based resin by using nano-silica particles. *IOP Conference Series: Earth and Environmental Science* 442(1): 012004.
- Ariffin, M.M., Aung, M.M., Abdullah, L.C. & Salleh, M.Z. 2020. Assessment of corrosion protection and performance of bio-based polyurethane acrylate incorporated with nano zinc oxide coating. *Polymer Testing* 87: 106526-106535.
- Cubides, Y. & Castaneda, H. 2016. Corrosion protection mechanisms of carbon nanotube and zinc-rich epoxy primers on carbon steel in simulated concrete pore solutions in the presence of chloride ions. *Corrosion Science* 109: 145-161.
- Di, H., Yu, Z., Ma, Y., Zhang, C., Li, F., Lv, L., Pan, Y., Shi, H. & He, Y. 2016. Corrosion-resistant hybrid coatings based on graphene oxide-zirconia dioxide/epoxy system. *Journal of the Taiwan Institute of Chemical Engineers* 67: 511-520.
- Ding, R., Zheng, Y., Yu, H., Li, W., Wang, X. & Gui, T. 2018. Study of water permeation dynamics and anti-corrosion mechanism of graphene/zinc coatings. *Journal of Alloys and Compounds* 748: 481-495.
- Harun, M.H. 2021. Characterization of hydrophobic UV-curable acrylated coating from palm oil based urethane acrylate (POBUA) for wood coating application. *Journal of Nuclear and Related Technologies* 18(02): 1-7.
- Huang, H-D., Ren, P-G., Chen, J., Zhang, W-Q., Ji, X. & Li, Z-M. 2012. High barrier graphene oxide nanosheet/poly(vinyl alcohol) nanocomposite films. *Journal of Membrane Science* 409-410: 156-163.
- Huang, X., Zhi, C., Lin, Y., Bao, H., Wu, G., Jiang, P. & Mai, Y-W. 2020. Thermal conductivity of graphene-based polymer nanocomposites. *Materials Science and Engineering: R: Reports* 142: 100577-100590.
- Jang, J-H., Oh, B. & Lee, E-J. 2021. Crystalline hydroxyapatite/graphene oxide complex by low-temperature sol-gel synthesis and its characterization. *Ceramics International* 47(19): 27677-27684.
- Khatoun, H., Iqbal, S., Irfan, M., Darda, A. & Rawat, N.K. 2021. A review on the production, properties and applications of non-isocyanate polyurethane: A greener perspective. *Progress in Organic Coatings* 154: 106124-106140.

- Kumar, S.S.A., Bashir, S., Ramesh, K. & Ramesh, S. 2021. New perspectives on graphene/graphene oxide based polymer nanocomposites for corrosion applications: The relevance of the graphene/polymer barrier coatings. *Progress in Organic Coatings* 154: 106215-106230.
- Liu, S., Tian, M., Yan, B., Yao, Y., Zhang, L., Nishi, T. & Ning, N. 2015. High performance dielectric elastomers by partially reduced graphene oxide and disruption of hydrogen bonding of polyurethanes. *Polymer* 56: 375-384.
- Mahidashti, Z., Shahrabi, T. & Ramezanzadeh, B. 2018. The role of post-treatment of an ecofriendly cerium nanostructure conversion coating by green corrosion inhibitor on the adhesion and corrosion protection properties of the epoxy coating. *Progress in Organic Coatings* 114: 19-32.
- Mellado, C., Figueroa Aguilar, T., Báez, R., Meléndrez, M. & Fernández, K. 2019. Effects of probe and bath ultrasonic treatments on graphene oxide structure. *Materials Today Chemistry* 13: 1-7.
- Mustapha, S.N.H., Md Nizam, M.N., Mohamad Isa, M.I., Roslan, R. & Mustapha, R. 2022. Synthesis and characterization of hydrophobic properties of silicon dioxide in palm oil based bio-coating. *Materials Today: Proceedings* 51: 1415-1419.
- Nam, K.H., Seo, K., Seo, J., Khan, S.B. & Han, H. 2015. Ultraviolet-curable polyurethane acrylate nanocomposite coatings based on surface-modified calcium carbonate. *Progress in Organic Coatings* 85: 22-30.
- Nik Salleh, N.G., Firdaus Yhaya, M., Hassan, A., Abu Bakar, A. & Mokhtar, M. 2011. Effect of UV/EB radiation dosages on the properties of nanocomposite coatings. *Radiation Physics and Chemistry* 80(2): 136-141.
- Nissenbaum, A., Greenfeld, I. & Wagner, H.D. 2020. Shape memory polyurethane - Amorphous molecular mechanism during fixation and recovery. *Polymer* 190: 122226-122234.
- Pourhashem, S., Vaezi, M.R., Rashidi, A. & Bagherzadeh, M.R. 2017. Exploring corrosion protection properties of solvent based epoxy-graphene oxide nanocomposite coatings on mild steel. *Corrosion Science* 115: 78-92.
- Prolongo, S.G., Moriche, R., Jiménez-Suárez, A., Sánchez, M. & Ureña, A. 2014. Advantages and disadvantages of the addition of graphene nanoplatelets to epoxy resins. *European Polymer Journal* 61: 206-214.
- Radovic, L.R., Mora-Vilches, C.V., Salgado-Casanova, A.J.A. & Buljan, A. 2017. Graphene functionalization: Mechanism of carboxyl group formation. *Carbon* 130: 340-349.
- Rajabi, M., Rashed, G.R. & Zaarei, D. 2015. Assessment of graphene oxide/epoxy nanocomposite as corrosion resistance coating on carbon steel. *Corrosion Engineering, Science and Technology* 50(7): 509-516.
- Said, H.M., Nik Salleh, N.G., Alias, M.S. & El-Naggar, A.W.M. 2013. Synthesis and characterization of hard materials based on radiation cured bio-polymer and nanoparticles. *Journal of Radiation Research and Applied Sciences* 6(2): 71-78.
- Sandhyarani, M., Prasadrao, T. & Rameshbabu, N. 2014. Role of electrolyte composition on structural, morphological and *in-vitro* biological properties of plasma electrolytic oxidation films formed on zirconium. *Applied Surface Science* 317: 198-209.
- Sang, L., Hao, W., Zhao, Y., Yao, L. & Cui, P. 2018. Highly aligned graphene oxide/waterborne polyurethane fabricated by *in-situ* polymerization at low temperature. *e-Polymers* 18(1): 75-84.
- Sarkar, M., Hasanuzzaman, M., Gulshan, F. & Rashid, A. 2020. Surface, mechanical and shape memory properties of biodegradable polymers and their applications. *Reference Module in Materials Science and Materials Engineering* 2: 1092-1099.
- Scully, J.R. & Hensley, S.T. 1994. Lifetime prediction for organic coatings on steel and a magnesium alloy using electrochemical impedance methods. *Corrosion* 50(9): 705-716.
- Sengupta, R., Bhattacharya, M., Bandyopadhyay, S. & Bhowmick, A.K. 2011. A review on the mechanical and electrical properties of graphite and modified graphite reinforced polymer composites. *Progress in Polymer Science* 36(5): 638-670.
- Seo, J., Jeon, G., Jang, E., Khan, S. & Han, H. 2011. Preparation and properties of poly(propylene carbonate) and nanosized ZnO composite films for packaging applications. *Journal of Applied Polymer Science* 122: 1101-1108.
- Suleiman, R.K., Kumar, A.M., Adesina, A.Y., Al-Badour, F.A., Meliani, M.H. & Saleh, T.A. 2020. Hybrid organosilicon-metal oxide composites and their corrosion protection performance for mild steel in 3.5% NaCl solution. *Corrosion Science* 169: 108637-108648.
- Thanh, N.T. 2022. Effect of graphene oxide on UV-thermo-humidity degradation of environmentally friendly alkyd composite coating. *Malaysian Journal on Composites Science and Manufacturing* 9(1): 1-10.
- Wan Rosli, W.D., Kumar, R.N., Mek Zah, S. & Hilmi, M.M. 2003. UV radiation curing of epoxidized palm oil-cycloaliphatic diepoxide system induced by cationic photoinitiators for surface coatings. *European Polymer Journal* 39(3): 593-600.

- Yahya, S., Othman, N.K. & Ismail, M.C. 2019. Corrosion inhibition of steel in multiple flow loop under 3.5% NaCl in the presence of rice straw extracts, lignin and ethylene glycol. *Engineering Failure Analysis* 100: 365-380.
- Yu, R., Wang, Q., Wang, W., Xiao, Y., Wang, Z., Zhou, X., Zhang, X., Zhu, X. & Fang, C. 2021. Polyurethane/graphene oxide nanocomposite and its modified asphalt binder: Preparation, properties and molecular dynamics simulation. *Materials & Design* 209: 109994-109100.
- Zulkafli, R., Othman, N.K., Rahman, I.A. & Jalar, A. 2014. Effect of rice straw extract and alkali lignin on the corrosion inhibition of carbon steel. *The Malaysian Journal of Analytical Sciences* 18(1): 204-211.
- Zuo, Y., Pang, R., Li, W., Xiong, J.P. & Tang, Y.M. 2008. The evaluation of coating performance by the variations of phase angles in middle and high frequency domains of EIS. *Corrosion Science* 50(12): 3322-3328.

*Corresponding author; email: insan@ukm.edu.my